

Article

E. coli MnmA Is an Fe-S Cluster-Independent 2-Thiouridylase

Moses Ogunkola , Lennart Wolff, Eric Asare Fenteng , Benjamin R. Duffus  and Silke Leimkühler * 

Department of Molecular Enzymology, Institute of Biochemistry and Biology, University of Potsdam, Karl-Liebknecht-Str. 24-25, 14476 Potsdam, Germany; ogunkola@uni-potsdam.de (M.O.); duffus@uni-potsdam.de (B.R.D.)

* Correspondence: sleim@uni-potsdam.de

Abstract: All kingdoms of life have more than 150 different forms of RNA alterations, with tRNA accounting for around 80% of them. These chemical alterations include, among others, methylation, sulfuration, hydroxylation, and acetylation. These changes are necessary for the proper codon recognition and stability of tRNA. In *Escherichia coli*, sulfur modification at the wobble uridine (34) of lysine, glutamic acid, and glutamine is essential for codon and anticodon binding and prevents frameshifting during translation. Two important proteins that are involved in this thiolation modification are the L-cysteine desulfurase IscS, the initial sulfur donor, and tRNA-specific 2-thiouridylase MnmA, which adenylates and finally transfers the sulfur from IscS to the tRNA. tRNA-specific 2-thiouridylases are iron–sulfur clusters (Fe-S), either dependent or independent depending on the organism. Here, we dissect the controversy of whether the *E. coli* MnmA protein is an Fe-S cluster-dependent or independent protein. We show that when Fe-S clusters are bound to MnmA, tRNA thiolation is inhibited, making MnmA an Fe-S cluster-independent protein. We further show that 2-thiouridylase only binds to tRNA from its own organism.

Keywords: tRNA; thiouridine; iron–sulfur cluster



Citation: Ogunkola, M.; Wolff, L.; Fenteng, E.A.; Duffus, B.R.; Leimkühler, S. *E. coli* MnmA Is an Fe-S Cluster-Independent 2-Thiouridylase. *Inorganics* **2024**, *12*, 67. <https://doi.org/10.3390/inorganics12030067>

Academic Editor: Nunziata Maio

Received: 26 January 2024

Revised: 19 February 2024

Accepted: 21 February 2024

Published: 23 February 2024



Copyright: © 2024 by the authors. Licensee MDPI, Basel, Switzerland. This article is an open access article distributed under the terms and conditions of the Creative Commons Attribution (CC BY) license (<https://creativecommons.org/licenses/by/4.0/>).

1. Introduction

The wobble nucleoside at position 34 of tRNA ubiquitously carries a thiomodification that enhances codon binding in vivo and is found frequently in all kingdoms of life [1]. The most conserved example is the wobble uridine of tRNA^{Lys, Gln, Glu} in bacteria that encompasses a sulfur-based modification at position 2 (s^2) and a side chain modification, e.g., 5-methoxyaminomethyl at position 5 (mnm^5). The genes involved in these modifications are conserved in eukaryotes from yeast to mammals, however a different set of genes, with a similar outcome is present in bacteria [2]. The modified uridine 34 is generally found in tRNAs that decode split codon-box family codons where the A- and G-ending codons encode a different amino acid than the U- and C-ending codons [3,4].

These modifications help to ensure the correct tRNA folding by stabilizing the conformation of the tRNA of the anticodon loop and facilitating their interactions with the aminoacyl-tRNA synthetase, thereby modulating mRNA decoding and ribosome processivity [5]. In yeast, it was shown that single tRNA mutants lacking either the mcm^5 or the s^2U34 modification have numerous phenotypes, including higher stress sensitivity and changes in temperature [1,6]. Higher temperatures and stress exposure were shown to lower the levels of s^2 thiomodifications. In humans and other eukaryotes, hypomodification is linked to neurological and mitochondrial disorders like type 2 diabetes and cancer [7,8]. These phenotypes arise from changes in the composition of the proteome caused by a reduced level of the translation of certain proteins. The lack of s^2 modification was shown to result in a higher density of ribosomes on mRNAs with repeats of AAA, CAA, and GAA codons [9,10]. Thereby, mcm^5s^2U34 at the first anticodon position is important for the exact base pairing interactions with purines with the third codon position harboring an A and G [11]. On the basis of the mnm^5s^2U34 -modified crystal structure of tRNA^{Lys} from *E. coli*,

that reads both Lys codons AAA and AAG, the s^2 group was revealed to be specifically involved in stacking with U35 and anticodon loop stabilization [12,13].

In *E. coli*, for the (c)mnm⁵s²U modification of tRNA^{Lys, Gln, Glu}, a specific sulfur-relay system has been identified, requiring the L-cysteine desulfurase IscS and the proteins TusA, TusBCD, TusE and MnmA [14]. Overall, the seven *E. coli* genes, namely *tusA*, *tusB*, *tusC*, *tusD*, *tusE*, *mnmA*, and *iscS*, were identified to be involved in the formation of s²U34 in specific tRNAs for Lys, Gln, and Glu. Among them, the *tusBCD* operon and their gene products form the TusBCD complex, composed of a ($\alpha\beta\gamma$)₂ dimer. In vitro, the most efficient 2-thiouridine formation is achieved using purified tRNA and the purified proteins IscS, TusA, and the TusBCD complex, in addition to TusE and MnmA [14]. TusA forms a complex with IscS and enhances its L-cysteine desulfurase activity two-fold. After the transfer of the persulfide group to Cys19 of TusA, TusA transfers sulfur further onto the Cys278 of TusD present in the TusBCD complex. Subsequently, TusE accepts the sulfur from TusD and transfers it to the Cys199 of MnmA. In vitro studies have shown that IscS can also directly transfer sulfur to MnmA but with a lowered efficiency relative to the TusBCD complex [14,15]. MnmA is a member of the adenosine 5'-triphosphate (ATP)-pyrophosphatase family and bears a PP-loop signature motif [15]. MnmA binds tRNA and ATP, and after binding, the tRNA is activated by an acyl-adenylated intermediate on U34. Subsequently, the persulfide sulfur of MnmA-Cys199 performs a nucleophilic attack on the acyl-adenylate intermediate, resulting in a formed tRNA thiocarbonyl group and a released adenosine 5'-monophosphate (AMP) molecule [15–17]. Finally, the persulfide of Cys199 in MnmA is reduced by Cys102, and s²U34-thiolated tRNA dissociates from MnmA. The newly formed disulfide bridge within MnmA has to be reduced before the next catalytic cycle. For the formation of the (c)mnm⁵ sidechain modification, the MnmG–MnmE complex and MnmC are essential (Figure 1). Here, both the mnm⁵ modification and the s²U modification in bacterial tRNAs were shown to be independently modified.

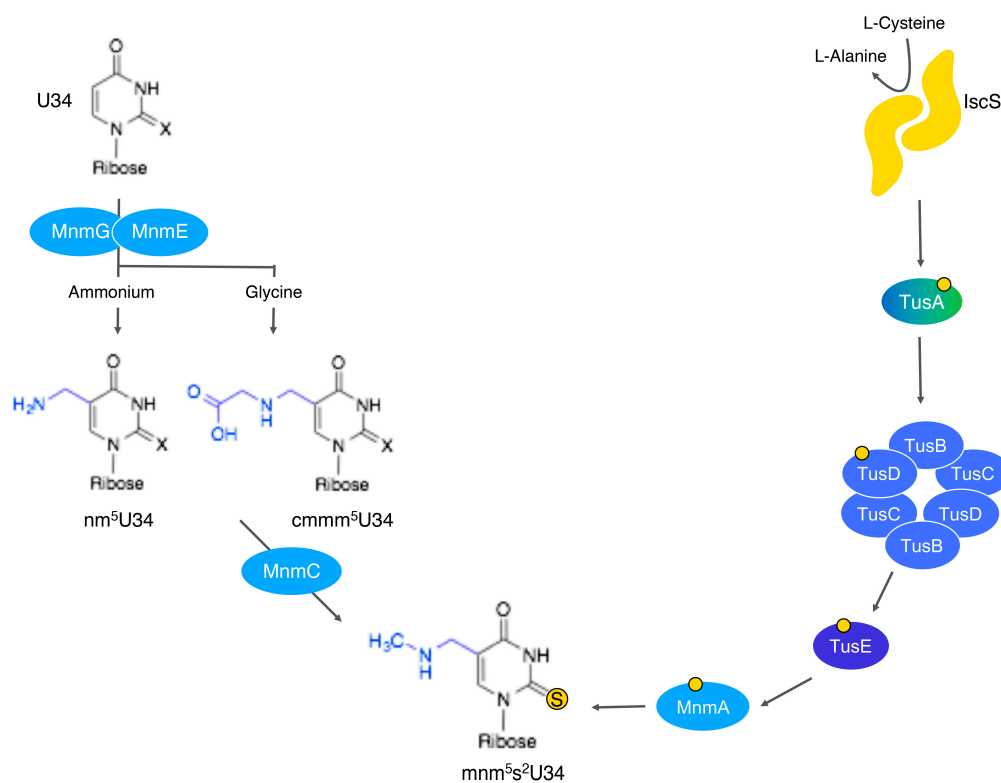


Figure 1. Formation of mnm⁵s²U34-modified tRNA in *E. coli*. Details are given in the text.

Two different routes of modification at the C5 position of uridine have been described, which are dependent on the substrate of MnmEG [18]. Either uridine on U34 is

converted into 5-methylaminomethyluridine (mnm^5) using ammonium as a substrate or 5-carboxymethylaminomethyluridine (cmnm^5) using the substrate glycine [18] (Figure 1). In turn, MnmC can convert mnm^5U into cmnm^5 using flavin adenine dinucleotide (FAD) as a cofactor, which is bound to the domain at the C-terminus. The N-terminal part of MnmC involved in donating a methyl group in a *S*-adenosylmethionine (SAM)-dependent reaction to nm^5U finally forms the mnm^5U modification.

The pathway for the thiomodification of $\text{mnm}^5\text{s}^2\text{U34}$ tRNAs present in bacteria resembles the human $\tau\text{m}^5\text{s}^2\text{U34}$ tRNA modification pathway present in the mitochondria [19]. In particular, the human MTU1 protein shares significant amino acid sequence homologies with bacterial MnmA [5]. In contrast, for the $\text{mcm}^5\text{s}^2\text{U34}$ modifications that are located in the cytosol, the human proteins MOCS3, URM1, CTU1, and CTU2 are essential [2,20]. This tRNA thiolation pathway is different from the $\text{mnm}^5\text{s}^2\text{U34}$ thiolation pathway in bacteria described above, using the proteins MOCS3, URM1, CTU1, and CTU2 instead. However, similar proteins are present in archaea and thermophilic bacteria [5,21,22]. While yeast mutant strains that contain an unmodified base at position U34 in tRNAs are not viable, the phenotype in yeast can be rescued by the overexpression of the respective hypomodified tRNAs [9]. This observation has led to the suggestion that the main function of the $\text{mcm}^5\text{s}^2\text{U34}$ modification is to improve the decoding efficiency of cognate codons and not to prevent missense errors. In bacteria, the role of (c) $\text{mnm}^5\text{s}^2\text{U}$ modifications is more complex than in eukaryotes. The overexpression of hypomodified tRNAs in bacteria does not improve the slow growth phenotype of *mnmA* or *mnmG* mutants but instead further reduces the slow growth of mutant strains [13]. It has been suggested that increased translational errors are consequentially due to the missing tRNA modifications [23]. This difference in translation correctness between *E. coli* and yeast has been noted earlier since missense errors are about 10-fold lower in yeast compared to *E. coli* [13]. Therefore, yeast might have evolved mechanisms to reduce missense errors that are not currently present in *E. coli* [24]. While the pathway of $\text{mnm}^5\text{s}^2\text{U34}$ formation was believed to be iron–sulfur Fe-S cluster-independent in *E. coli* [25,26], the MnmA homologous proteins NCS2 (yeast) and CTU1 (humans) are Fe-S-cluster-dependent proteins [25]. Here, analysis of the MnmA sequences from bacteria and eukaryotes revealed that the MnmA homologs can be divided into two groups: one that contains a conserved C-DXXC-C motif (D-type) and one that contains a conserved CC-CXXC-C motif (C-type) [5]. In addition, the D-type enzymes are believed to be Fe-S cluster-independent, while the C-type ones are classified to be Fe-S-cluster-dependent [5].

In contrast, the tRNA thiomodifications of 2-thiocytidine at position 32 ($\text{s}^2\text{C32}$) and of 2-methylthio-N⁶ isopentenyladenosine at position ($\text{ms}^2\text{i}^6\text{A37}$) for certain tRNAs are Fe-S cluster-dependent (Figure 2) [25]. In *E. coli*, these tRNA modifications involve the proteins TtcA for the $\text{s}^2\text{C32}$ modification and MiaB for the $\text{ms}^2\text{i}^6\text{A37}$ modification (Figure 2). TtcA binds one [4Fe-4S] cluster, while MiaB binds two [4Fe-4S] clusters and is a member of the radical SAM superfamily of proteins [27,28]. In contrast, the $\text{s}^4\text{U8}$ and (c) $\text{mnm}^5\text{s}^2\text{U34}$ thiomodifications are so far described to be Fe-S cluster-independent in *E. coli* [2,25,26] (Figure 2).

E. coli MnmA was believed to be an Fe-S cluster-independent protein based on the fact that no Fe-S cluster was identified in the crystal structure of the protein [16,17]. Recently, a report describing the purification of a [4Fe-4S] cluster containing the MnmA protein isolated under anaerobic conditions from *E. coli* reported that this [4Fe-4S] cluster is essential for its activity [29]. However, this report contradicts our previous published data, where we showed that by using an *E. coli iscS* mutant strain complemented with a *sufS*-expressing plasmid, the Fe-S cluster biosynthesis was rescued, and this strain was able to produce $\text{s}^2\text{C32}$ or $\text{ms}^2\text{i}^6\text{A37}$ -modified tRNAs, but not $\text{s}^4\text{U8}$ and (c) $\text{mnm}^5\text{s}^2\text{U34}$ tRNAs [26]. Our previous results showed clearly the differentiation of two tRNA thiolation pathways in *E. coli* as being either Fe-S cluster-dependent or independent, as initially described by Suzuki [25]. To clarify the contradiction with the recent publication by Zhou et al. [29], we aimed to investigate the activity of the Fe-S cluster containing MnmA under our conditions.

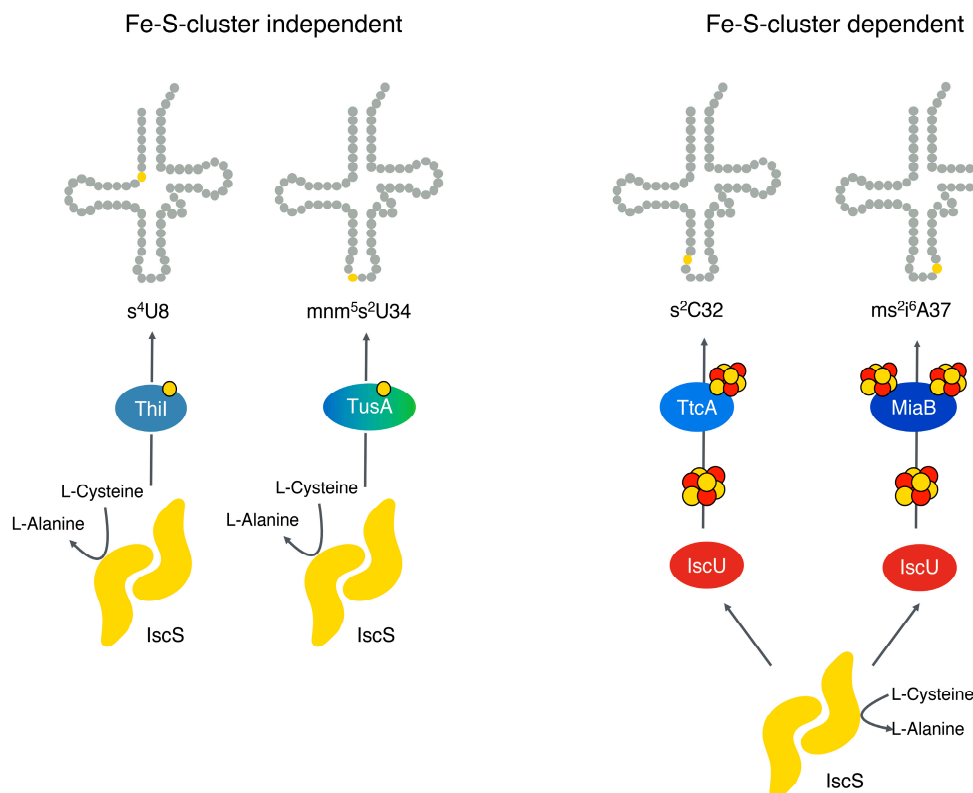


Figure 2. The different tRNA thiomodification pathways and their groupings into Fe-S-cluster-dependent and independent pathways. Details are given in the text.

2. Results

2.1. Purification of *E. coli* MnmA under Anaerobic Conditions and Reconstitution with a [4Fe-4S] Cluster

E. coli MnmA with an N-terminal His₆-tag was purified under aerobic (MnmA+O₂) and anaerobic conditions (MnmA-O₂) using Ni-NTA chromatography. As purified, the UV-Vis spectrum for each purification condition of MnmA (Figure 3A, orange and blue traces, respectively) revealed that hardly any Fe-S clusters were bound to the two proteins, which was supported by a lack of detected Fe by inductively coupled plasma optical emission spectroscopy (ICP-OES). Similarly, the UV-Vis spectrum of MnmA isolated from an *E. coli* *iscS*-mutant strain expressed aerobically was virtually identical to the MnmA+O₂ expressed in the *E. coli* BL21 strain (Figure 3A, dashed trace), reflecting a similar lack of Fe-S clusters bound.

To assess MnmA's ability to bind an Fe-S cluster, we carried out an *in vitro* reconstitution of the Fe-S cluster via the treatment of the aerobically and anaerobically purified proteins with ferrous iron and L-cysteine in the presence of the L-cysteine desulfurase IscS as a source of sulfur under anaerobic conditions. In contrast to as-purified MnmA, the Fe-S cluster reconstitution of MnmA (referred to as MnmA-rec) resulted in a brownish protein with apparent Fe bound, yielding Fe numbers of 2.5 ± 0.1 and a 2.8 ± 0.2 Fe/MnmA protomer for the MnmA+O₂ rec and MnmA-O₂ rec samples, respectively. Respective UV-Vis spectra exhibited a broad absorption band at 410 nm that was reminiscent of a protein-bound [4Fe-4S] cluster (Figure 3A, green and purple traces). Size exclusion chromatography was performed on the MnmA-rec under anaerobic conditions, leading to a homogenous, monomeric protein that was similar to the as-purified enzyme lacking bound Fe (Figure 3B). In turn, the presence of a bound Fe-S cluster appeared to not influence the oligomerization state of the protein.

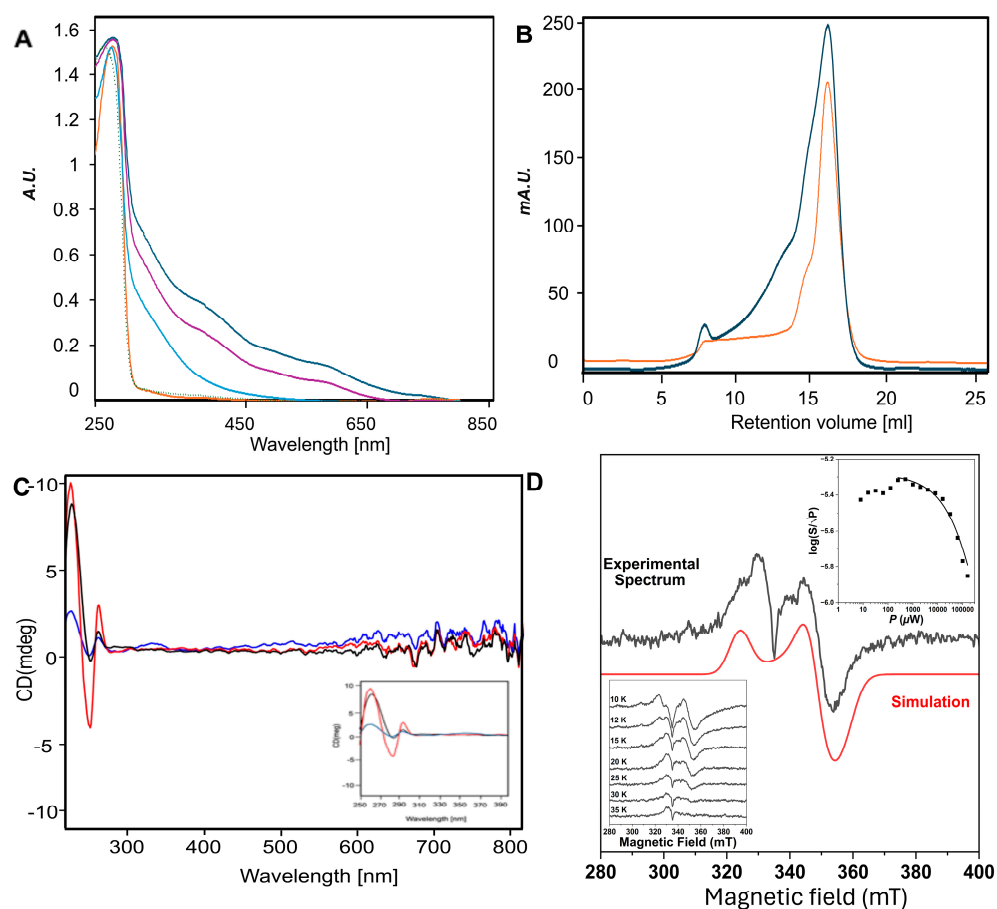


Figure 3. Spectroscopic analysis of purified MnmA. **(A)** UV-visible absorption spectra of 50 μM MnmA expressed in the *E. coli* BL21 DE3 strain purified under aerobic (orange trace) or anaerobic (blue trace) conditions. Both proteins were in vitro reconstituted with Fe-S clusters. The UV-Vis spectra of aerobically purified and reconstituted MnmA (green trace), and anaerobically purified and reconstituted MnmA (purple trace) are also shown. For reference, MnmA expressed aerobically in the *E. coli iscS* mutant strain is depicted as a dashed trace. All UV-Vis spectra were recorded in 50 mM HEPES, 150 mM KCl, pH 7.5 buffer. **(B)** Analytical size exclusion chromatography of MnmA. Runs were performed with 50 μM of aerobically purified MnmA+O₂ (orange trace) and MnmA-rec (blue trace) on a Superdex 200 column equilibrated 50 mM HEPES, 150 mM KCl, pH 7.5 buffer. The elution signal was recorded at 280 nm. SEC for the MnmA-rec sample was performed in an anaerobic chamber (<10 ppm O₂). **(C)** CD spectra of MnmA. Spectra were recorded at a 1.00 mm path length in a light-protected quartz cuvette with a Jasco-J715 CD spectrometer equipped with a thermoelectric temperature-controlled cuvette holder. The CD was recorded at a range of 250–800 nm using a step size of 1 nm with a signal averaging time of 4 s at each wavelength step. In total, 500 μL of MnmA at a concentration of 0.25 mg/mL was used. Aerobically purified MnmA+O₂ (blue trace), reconstituted MnmA-O₂-rec (black) and anaerobically purified and reconstituted MnmA-rec (red trace) were measured. The inset is a zoom-in of the region 200–350 nm. **(D)** CW X-band EPR spectra of the Fe-S cluster bound to MnmA-rec. The main panel depicts 244 μM of MnmA-rec that was reduced with 10 mM Na₂S₂O₄ in 10 mM Tris-HCl, 50 mM KCl, 12 mM MgCl₂, pH 8.5 buffer. The spectral simulation is depicted in bold red color. The spectrum in the main panel was obtained at 15 K, with a microwave frequency of 9.401 GHz, a modulation amplitude of 10 G, a microwave power of 159 μW , and a modulation frequency of 100 kHz. The top right inset panel depicts a power relaxation curve for the Na₂S₂O₄-reduced Fe-S cluster signal measured at 12 K. The bottom left inset panel depicts a temperature relaxation curve for the sample, measured at 159 μW of microwave power. The spectral simulation of the Fe-S cluster above gave the associated *g*-tensor parameters with the following *g*-values: 2.073, 1.928, 1.885 ($g_{\text{av}} = 1.964$; $g_{\text{aniso}} = 0.188$; $g_{\text{rhomb}} = 0.772$); the *g*-strain is as follows: 49.9, 42.7, 50.0 ($\times 10^{-3}$).

The binding of a [4Fe-4S] cluster to MnmA could be confirmed by CD and EPR spectroscopies. First, CD spectroscopy appeared to exclude the presence of [2Fe-2S] clusters, in that the CD spectrum showed minimal spectral features in the region of 300–700 nm (Figure 3C). This appeared to indicate the presence of a bound [4Fe-4S] cluster that was CD-silent (Figure 3C) since in the case a [2Fe-2S] cluster was bound, a characteristic spectrum with spectral features would be expected [30]. To confirm this observation, EPR spectroscopy was performed on MnmA-rec (Figure 3D). The reduction in the Fe-S cluster reconstituted MnmA with 10 mM of Na₂S₂O₄ resulted in the detection of a very broad paramagnetic resonance and a similar reminiscent of a bound Fe-S cluster. Measurements at 15 K and 159 μW microwave power resulted in a signal corresponding to 0.13 spins/protein, reflecting a partial reduction in the bound Fe-S cluster. To characterize the behavior of this Fe-S cluster better, the relaxation properties of the bound Fe-S cluster were assessed. At 12 K, the Fe-S cluster was largely resistant to microwave power, with a $P_{1/2}$ observed to be >100 mW and a P_M of approximately 100 μW of microwave power. By comparison, under non-saturating power conditions, the Fe-S cluster appeared completely spin-relaxed at temperatures above 30 K. The spectral simulation of the Fe-S cluster at 15 K and 159 μW microwave power gave g -values of 2.073, 1.928, 1.885 ($g_{av} = 1.964$; $g_{aniso} = 0.188$; $g_{rhomb} = 0.772$) with a substantial g -strain (49.9, 42.7, 50.0 ($\times 10^{-3}$)), largely similar to other [4Fe-4S]-coordinating Fe-S cluster proteins after in vitro Fe-S cluster reconstitution.

2.2. The [4Fe-4S] Cluster Inhibits the tRNA Thiolation Activity of *E. coli* MnmA

The activity of purified aerobic MnmA+O₂ and MnmA-rec were tested in an in vitro tRNA thiolation assay using the purified proteins and tRNA isolated from a $\Delta iscS$ mutant strain, to exclude the copurification of Fe-S clusters with the tRNA and to ensure the complete lack of mnm⁵s²U34-modified nucleosides. For in vitro thiolation, purified tRNA was incubated with MnmA+O₂ or MnmA-rec in the presence of IscS, L-cysteine, pyridoxal 5'-phosphate (PLP), Mg-ATP, and dithiothreitol (DTT). tRNA was cleaved into nucleosides by P1 treatment, and the resulting nucleosides were separated by HPLC and identified by their characteristic UV-Vis spectra. The amount of mnm⁵s²U34 nucleosides was normalized to the pseudouridine peak (Figure 4). tRNA from the $\Delta iscS$ strain and from the corresponding parental strains (BW25113 or MC2061) were used as controls. The results showed that when using aerobically purified MnmA+O₂, mnm⁵s²U34-modified nucleosides were produced, while when using anaerobically purified and reconstituted MnmA-rec, no thiomodified nucleosides were detected (Figure 4A).

This shows that the presence of [4Fe-4S] clusters on MnmA might rather inhibit the transfer of sulfide to the tRNA. To verify that MnmA without an Fe-S cluster was active, purified MnmA from a $\Delta iscS$ -mutant strain was compared. MnmA purified from the $\Delta iscS$ strain should be devoid of Fe-S clusters (Figure 3A) and therefore should be inactive for mnm⁵s²U34 production in the case that Fe-S clusters are required for thiomodification. However, we were able to detect mnm⁵s²U34-modified thionucleosides using MnmA purified from the $\Delta iscS$ mutant strain in conjunction with the tRNA from the $\Delta iscS$ strain (Figure 4B), showing that Fe-S cluster-free MnmA is active in mnm⁵s²U34 formation.

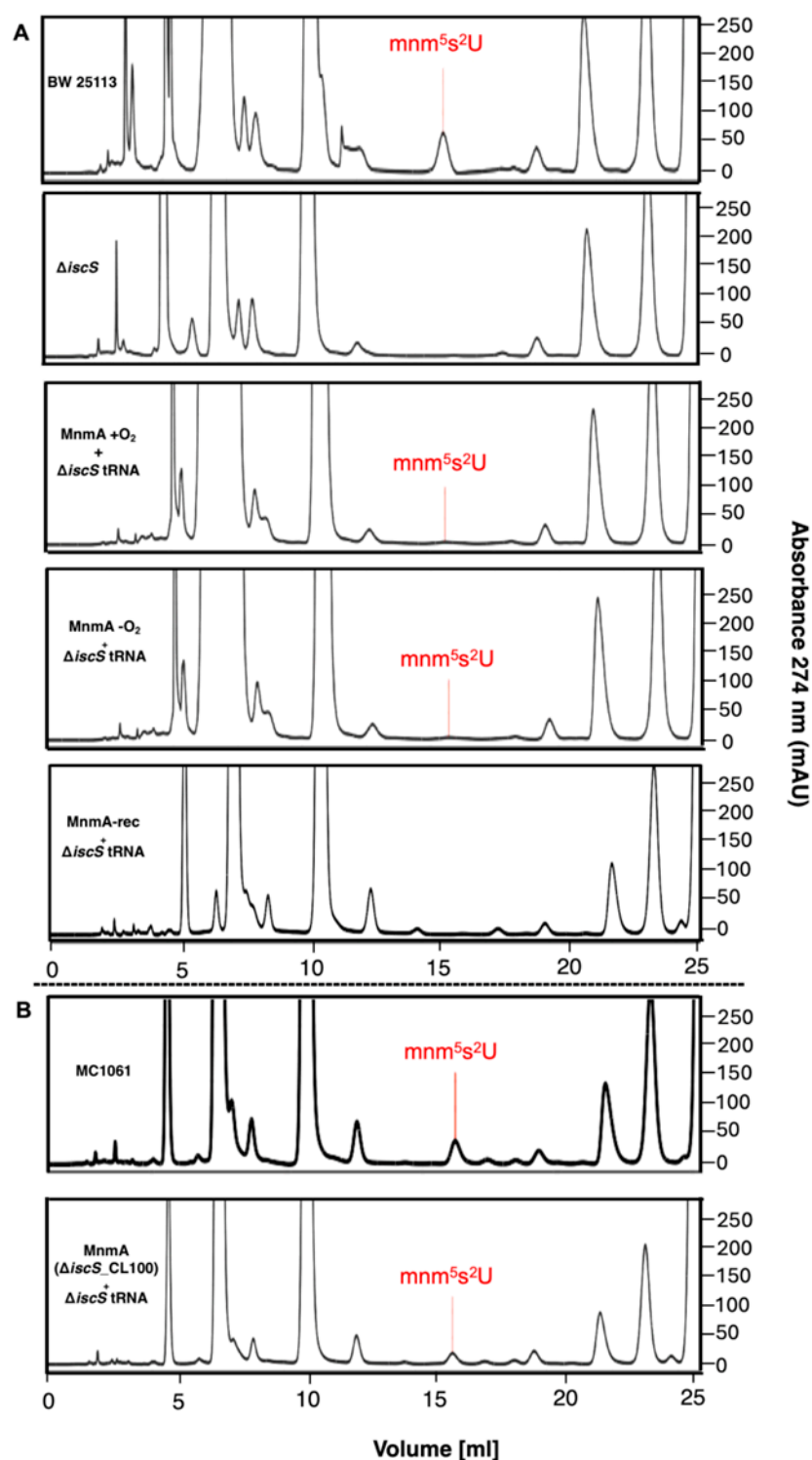


Figure 4. In vitro synthesis of $mnm^5s^2U_{34}$ -modified nucleosides in tRNA. (A) Chromatogram of the separated nucleosides. In total, 300 μ g of tRNA purified from the *E. coli* $\Delta iscS$ strain were incubated with 150 μ M of aerobically purified MnmA+O₂, anaerobically purified MnmA, reconstituted MnmA-rec or (B) MnmA purified from the CL100_ $\Delta iscS$ strain in the presence of 100 μ M IscS, 1 mM L-cysteine, 20 μ M PLP, 1 mM ATP and 1 mM DTT. tRNAs from each reaction were extracted, and 200 μ g of the extracted tRNAs were digested and separated on an HPLC C18 reversed-phase column (LiCrospher 100, 5 m particle size, 250 4.6 mm) *E. coli* BW25113, MC1061, and $\Delta iscS$ tRNA were measured as controls. Representative chromatograms ($n = 3$) (n represents the number of biological replicates) are shown.

2.3. MnmA-rec Is Able to Bind tRNA

To further identify the reason why the MnmA-rec protein was inactive for mnm⁵s²U34 thionucleoside formation, we first tested whether the binding of tRNA is impaired by the [4Fe-4S] cluster. In particular, we tested whether the proteins are able to bind tRNA to protect them from proteolysis. In turn, MnmA+O₂ and MnmA-rec were incubated with tRNA purified from the *E. coli* Δ iscS strain and were incubated with various amounts of trypsin. The proteins were not incubated with tRNA and were completely degraded by trypsin treatment (Figure 5).

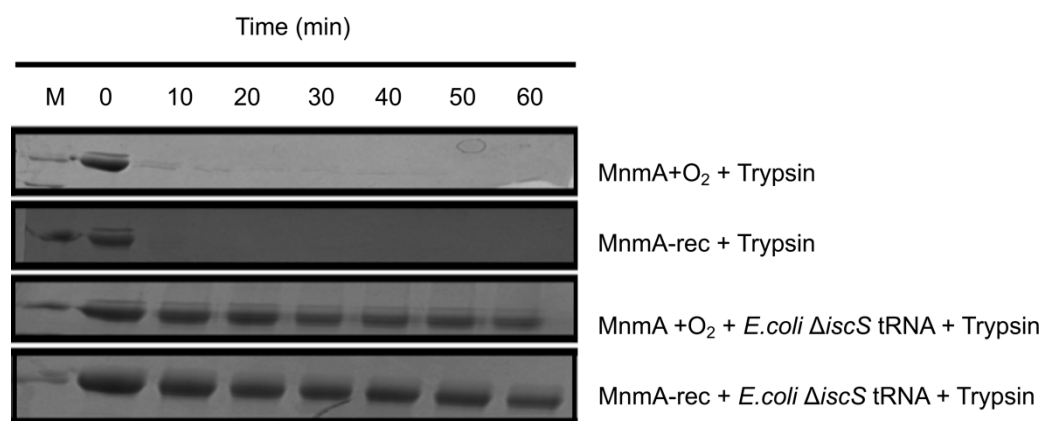


Figure 5. Interaction studies of MnmA with *E. coli* tRNA. The 10% SDS polyacrylamide gels stained with Coomassie brilliant blue. Trypsinolysis assay was carried out with either 0.13 mg/mL of MnmA+O₂ or MnmA-rec in the presence of 2.6 μ g/mL of trypsin, and in the presence or absence of 1.5 mg/mL of *E. coli* Δ iscS tRNA. Samples were taken at indicated time point intervals and were separated by SDS-PAGE. MnmA+O₂ and reconstituted MnmA-rec were preincubated with *E. coli* Δ iscS tRNA before the addition of trypsin.

Both MnmA+O₂ and MnmA-rec incubated with tRNA were not degraded by trypsin, showing that both proteins were able to bind tRNA to protect them from trypsinolysis (Figure 5). Therefore, the Fe-S cluster did not inhibit the binding of tRNA to MnmA.

2.4. The Fe-S Cluster on MnmA Impairs the Interaction of IscS

Since MnmA and IscS are predicted to interact for sulfur transfer to form the s²U34 group on tRNA, we investigated the interaction of MnmA+O₂ and MnmA-rec with *E. coli* IscS. SPR measurements were employed for the real-time detection of specific interactions using the purified proteins. MnmA+O₂ and MnmA-rec were immobilized on a CM5 chip via amine coupling. As binding partners, we used purified IscS (0.3 μ M to 20 μ M). The resulting sensograms reflected the association and dissociation of the two proteins, which confirmed the interaction between MnmA+O₂ and IscS and MnmA-rec with IscS. Kinetic data were fitted on the plot based on a simple 1:1 binding model. The mean K_D values obtained from two independent SPR measurements for the protein pairs are listed in Table 1. BSA served as a negative control and showed no interaction with IscS since no RUs were detected. An interaction between either MnmA+O₂ or MnmA-rec with IscS was detected; however, the K_D value for MnmA-rec was two-fold higher than the K_D of MnmA+O₂ with IscS. This reflects how MnmA-rec interacts with IscS with a lower affinity, showing that the [4Fe-4S] cluster likely interferes with the binding of IscS to MnmA, thereby likely resulting in an impaired sulfur transfer to the tRNA. An interaction of IscS with itself was detected, likely reflecting an interaction between the monomers present from the IscS purification.

Table 1. SPR analysis using the BiacoreT200 system. The kinetic constants (K_D) were determined using BIAcore T200 analysis software.

Immobilized Protein ^a	Protein Partners ^c	K_D ^d (μ M)	Rmax (RU) ^b
IscS	BSA	0.99 ± 1.66	N.D
	IscS	3.08 ± 1.34	39.713
	MnmA+O ₂	5.12 ± 1.66	62.236
	MnmA-rec	11.15 ± 5.92	33.903

^a Proteins were immobilized via amine coupling; ^b RU, resonance units; ^c Proteins were injected using the KINJECT protocol, injecting samples at a concentration range of 0.4 to 20 μ M. Cells were regenerated by the injection of 20 mM of HCl; ^d K_D values were obtained by global fitting procedures for 1:1 binding. Mean of ($n = 3$) (n represents the number of biological replicates) are shown. N.D. not detectable.

2.5. MnmA-rec Does Not Transfer Sulfur to tRNA

To analyze whether sulfur transfer to tRNA is indeed impaired in the presence of the [4Fe-4S] cluster on MnmA, we used ³⁵S-labeled L-cysteine and analyzed the transfer to tRNA using IscS, Mg-ATP, L-³⁵S-cysteine, MnmA+O₂ or MnmA-rec. The labeled tRNAs was detected after separation on a urea-PAGE via radio imaging. The result showed that no labeled tRNA was detected using the MnmA-rec protein, while labeling was present using the aerobically purified MnmA+O₂ (Figure 6B).

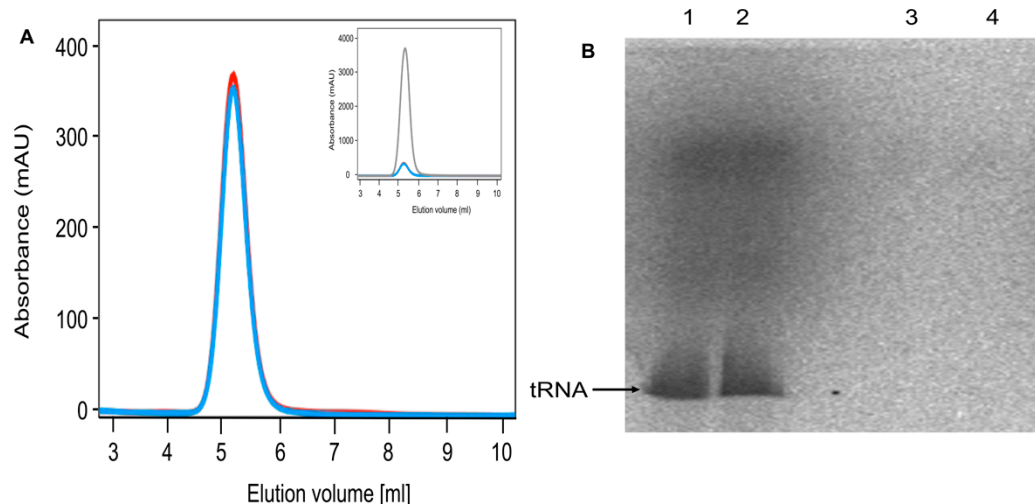


Figure 6. Adenylation and sulfuration of tRNA by MnmA. Aerobically purified MnmA+O₂ and MnmA-rec were incubated in 50 mM Tris-HCl, 150 mM MgCl, pH 7.5 buffer with ATP and PP_i in the presence of tRNA. **(A)** Amount of AMP formed and separated on a C18-RP HPLC column. Nucleosides were detected at 260 nm. AMP standard control (gray trace) and AMP formed by MnmA+O₂ (blue trace) and MnmA-rec (red trace). The inset shows the AMP standard relative to the AMP formed using MnmA. **(B)** 5% Urea gel after radio imaging. Incubation mixtures were separated on the urea gel containing the following: 300 μ g tRNA, 10 μ Ci ³⁵S-labeled L-cysteine, either 150 μ M MnmA+O₂ (lanes 1 and 2) or 150 μ M of MnmA-rec (lanes 3 and 4), 1 mM DTT, 1 mM ATP, and 20 μ M PLP. The tRNA was extracted and separated on the urea gel.

In addition, ATP binding was not impaired in the MnmA-rec enzyme; the same amount of AMP production for both MnmA proteins was observed by analyzing the ATP cleavage activity of the protein (Figure 6A).

2.6. SufS Is Not Able to Rescue *mnm*⁵*s*²U34 tRNA Modification in Conjunction with MnmA

To verify our previous results showing that SufS rescues Fe-S-dependent tRNA thiolation but not Fe-S-independent tRNA thiolation in *E. coli*, we used the Δ *iscUA*/ Δ *sufABCDSE* strain, which is completely devoid of Fe-S cluster formation and was also used in the report

by Zhou et al. [29]. We complemented the strain with a plasmid expressing the complete *suf* operon so that Fe-S cluster assembly could be restored in the strain. While the strain was mainly impaired in the s^2C32 and ms^2i^6A37 nucleoside formation, mnm^5s^2U34 - and s^4U8 -modified nucleosides were detectable in this strain (Figure 7A).

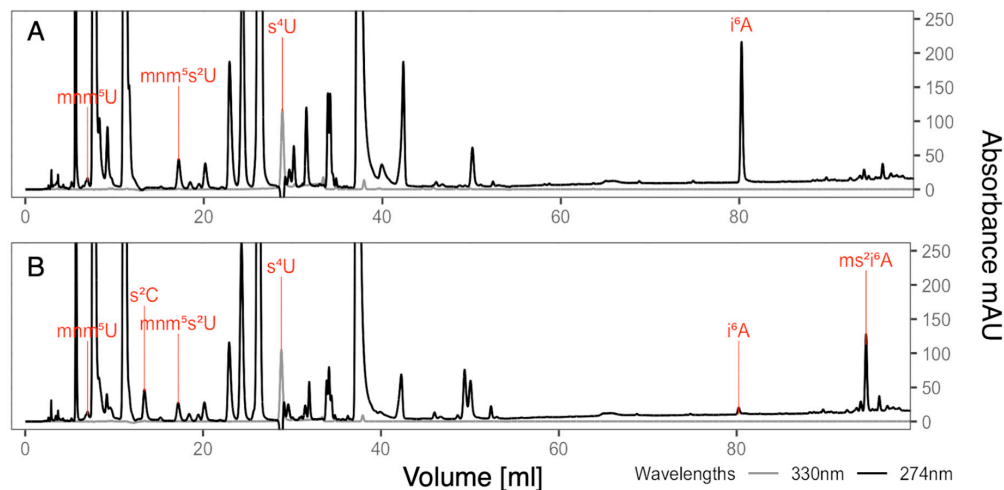


Figure 7. HPLC elution profile of separated tRNA nucleosides. The figure depicts (A) tRNA purified from the $\Delta iscUA/\Delta sufABCDSE$ strain and (B) tRNA purified from the $\Delta iscUA/\Delta sufABCDSE$ strain, which was transformed with the plasmid pPH151 expressing the *E. coli* *sufABCDSE* operon. The peaks of various modified nucleosides were labeled red. The respective nucleosides were identified by their characteristic UV-Vis absorption spectra. Representative chromatograms ($n = 3$) (n represents the number of biological replicates) are shown.

After the complementation of this strain with a plasmid expressing the *sufABCDSE* operon, the s^2C32 - and ms^2i^6A37 -modified nucleoside formation was rescued, and modified nucleosides were readily detectable (Figure 7B). By contrast, the concentration of the mnm^5s^2U34 - and s^4U8 -modified nucleosides remained constant and were not rescued by the introduction of the *suf* operon, showing their independence from Fe-S cluster formation in the cell.

2.7. Complementation of the $\Delta mnmA$ Mutant Strain with Human MTU1 and CTU1

Since *E. coli* MnmA and human MTU1 are functional homologs, we tested whether human MTU1 can complement the *E. coli* $\Delta mnmA$ mutant strain. While the growth defect of the *E. coli* $\Delta mnmA$ strain was rescued by plasmid-expressing *E. coli* *mnmA* (Figure 8A), human MTU1 or CTU1 were unable to rescue the growth defect of the mutant strain (Figure 8B,C), showing that despite their amino acid sequence identities of 44% and 23%, respectively, species-specific differences in the role of the proteins acting as tRNA thiouridylases were observed.

We further tested whether the proteins could bind to tRNA from other species. We were able to show that *E. coli* MnmA is unable to bind to human tRNA (Figure 9C). Human MTU1 is unable to bind to *E. coli* tRNA (Figure 9B). By contrast, human tRNA was found to bind to MTU1 (Figure 9C).

To further investigate whether the side-chain modification is important for the binding of the respective tRNA to the thiouridylase from the same species, we tested the binding of tRNA isolated from the $\Delta mnmE$ or $\Delta mnmG$ mutant strains to either MnmA or MTU1, which should be devoid of the *mnm* modification. While $\Delta mnmE$ tRNA protected the *E. coli* MnmA protein from proteolysis (Figure 9A), it did not protect the MTU1 protein from proteolysis (Figure 9B), showing that factors other than the side chain modification influence species-specific tRNA binding to the thiouridylase. By comparison, MTU1 was protected from trypsinolysis by human tRNA (Figure 9C).

To further investigate why *E. coli* tRNA was not thiolated by human MTU1, and why human tRNA is not thiolated by MnmA, we tested the sulfur transfer to the respective tRNA using the *E. coli* IscS protein and the human NFS1 protein with either *E. coli* MnmA or human MTU1. The results of in vitro tRNA thiolation showed that IscS was unable to transfer the sulfur to *E. coli* tRNA using human MTU1, and that human NFS1 was unable to transfer sulfur to human tRNA using *E. coli* MnmA (Figure 10). This shows that the sulfur transfer of L-cysteine desulfurase to 2-thiouridylase seemed to be tRNA species-specific. NFS1 was able to transfer the sulfur to MTU1 when human tRNA was used, and IscS was able to transfer the sulfur to MnmA when *E. coli* tRNA was used, but only MnmA+O₂ could transfer the sulfur to *E. coli* tRNA, not MnmA-rec.

Therefore, species-specific sulfur transfer to the respective tRNA is based on differences in the tRNA and not based on the participatory L-cysteine desulfurase. The Fe-S clusters on MnmA again inhibited the sulfur transfer.

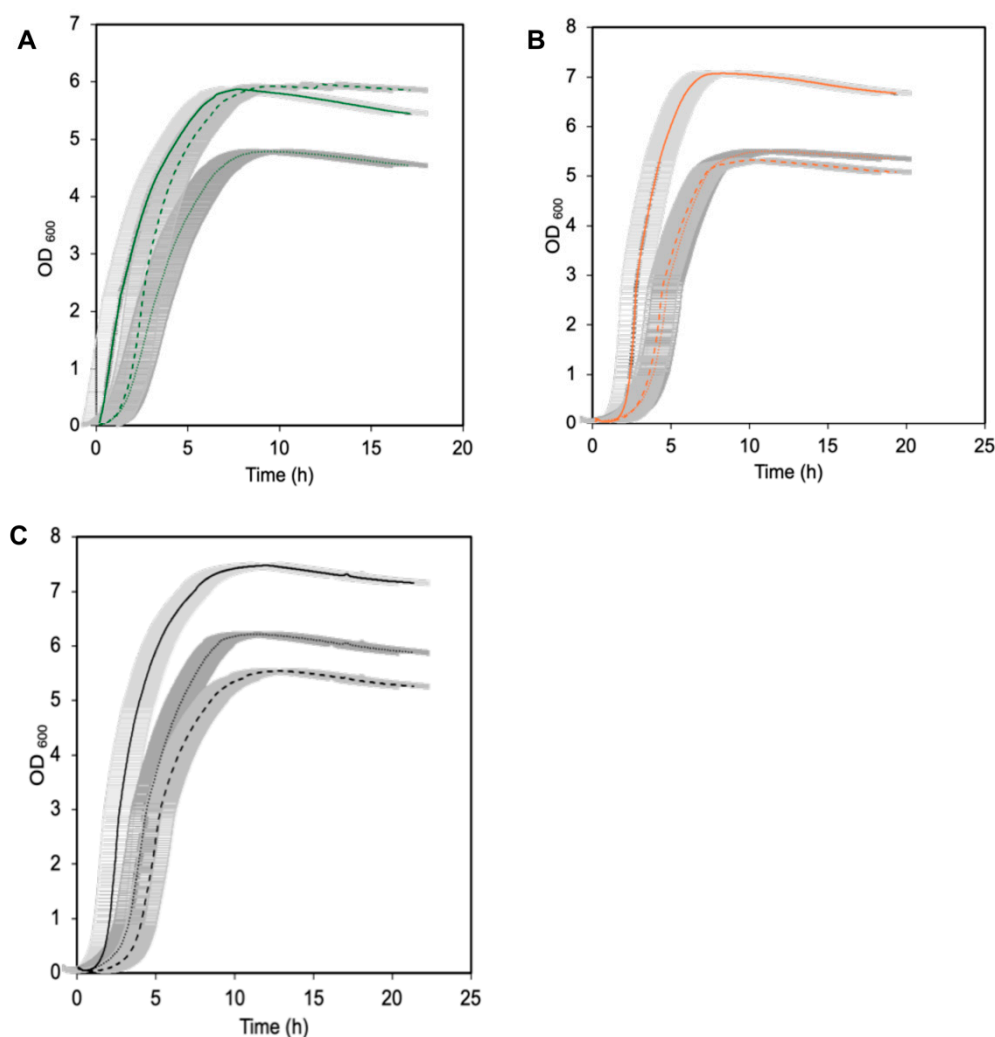


Figure 8. (A) Growth curves of *E. coli* BW25113 (solid line), the $\Delta mnmA$ strain (dotted line), and the strain transformed with plasmid-expressing *E. coli* mnmA (dashed line). (B) Growth curves of *E. coli* BW25113 (solid line), the $\Delta mnmA$ strain (dotted line), and the strain strains transformed with plasmid-expressing human MTU1 (dashed line). (C) Growth curves of *E. coli* BW25113 (solid line), the $\Delta mnmA$ strain (dotted line), and the strain strains transformed with plasmid-expressing human CTU1 (dashed line). The OD₆₀₀ was recorded constantly over 25 h. Growth curves represent the means ($n = 3$) (n represents the number of biological replicates); error bars are shown.

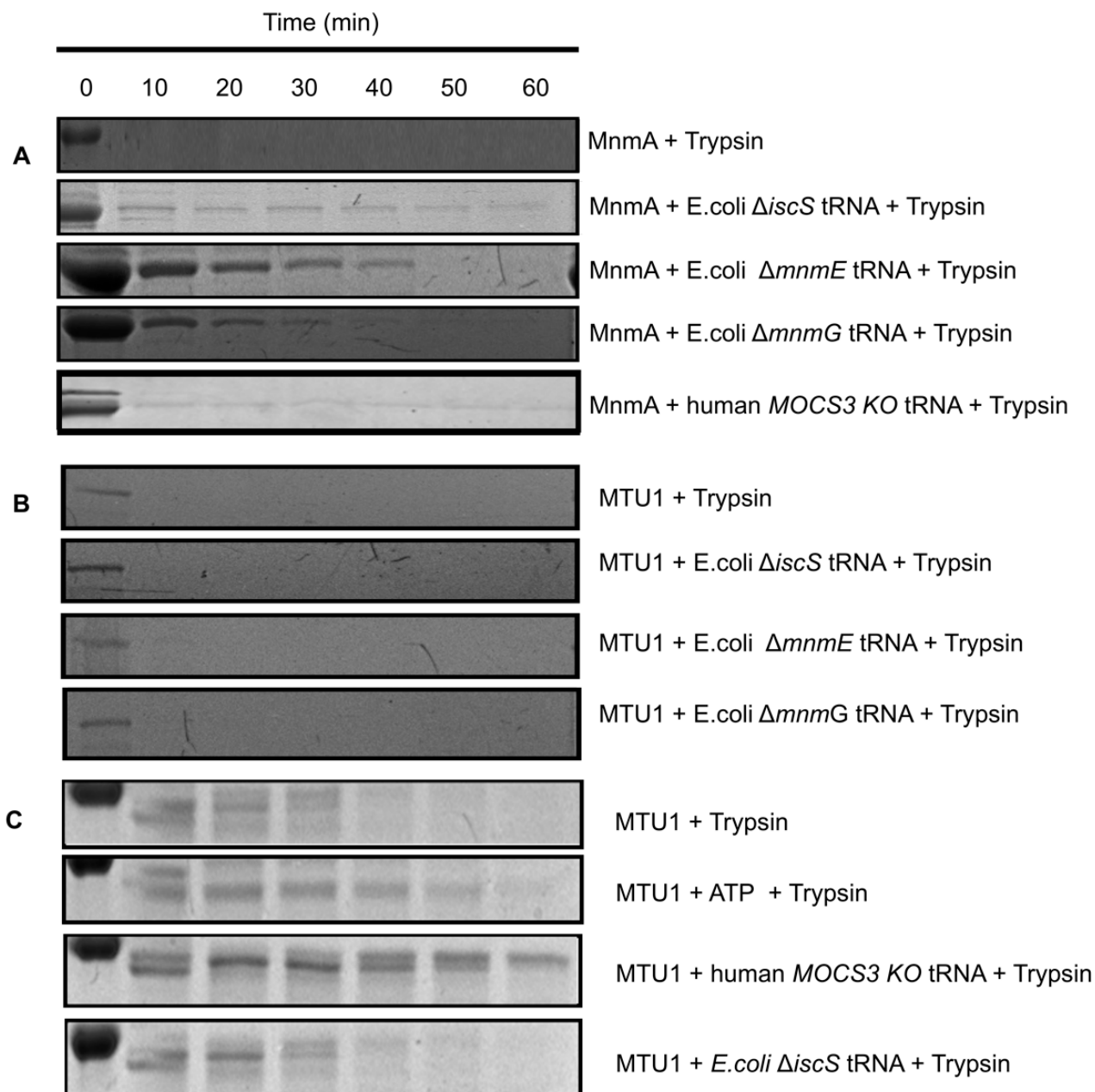


Figure 9. Interaction studies of MTU1 and MnmA with tRNA purified from *E. coli* Δ mnmE cells, Δ iscS cells, or human tRNA. Separation was performed on 10% acrylamide gels stained with Coomassie brilliant blue. The trypsinolysis assay was carried out with 0.13 mg/mL of either MnmA or MTU1 in the presence of 2.6 μ g/mL trypsin, with 1.5 mg/mL of either *E. coli* tRNA or human tRNA, with incubation at 37 °C for 1 h. Samples were taken at indicated intervals and were prepared by SDS-PAGE. (A) MnmA-rec was incubated with tRNA *E. coli* Δ mnmE or Δ mnmG cells or human tRNA. (B) Human MTU1 was incubated with tRNA from *E. coli* Δ mnmE or Δ mnmG strains. (C) Human MTU1 was incubated with tRNA from HEK293T MOCS3KO cells.

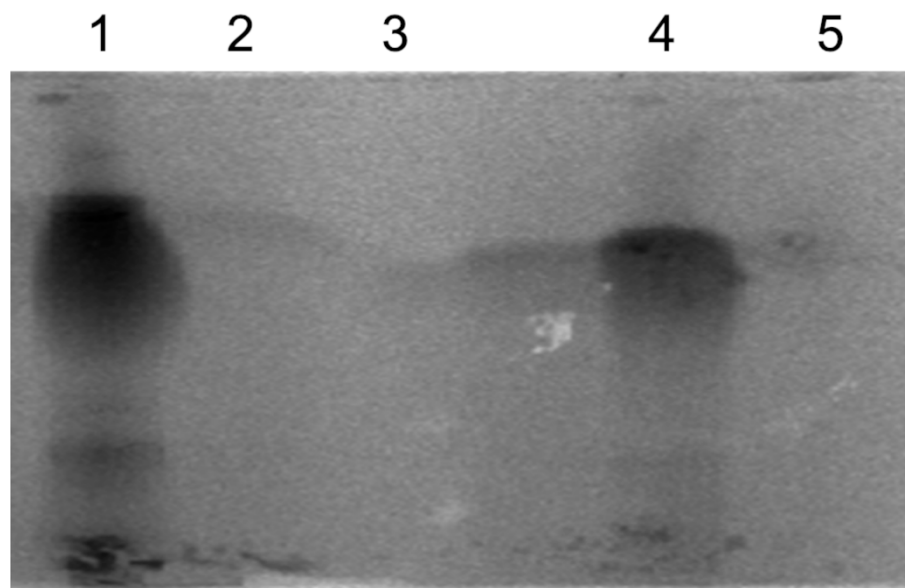


Figure 10. In vitro ^{35}S persulfide transfer between NFS1, IscS, MTU1 and MnmA. In lanes 1–3, 150 μM of IscS was incubated with 300 μM of either MnmA+O₂ (1), MnmA-rec (2) or MTU1 (3) in the presence of 2 μCi L- ^{35}S -cysteine for 1 h at 37 °C and 150 μM tRNA purified from *E. coli*. In lanes 4–5, 150 μM NFS1 was incubated with either 300 μM MTU1 (4), or MnmA+O₂ (5) in the presence of 2 μCi L- ^{35}S -cysteine for 1 h at 37 °C and 150 μM tRNA purified from human HEK 293T cells. The resulting solutions were mixed with an SDS loading buffer without boiling and were separated on a 12% SDS–polyacrylamide gel under nonreducing conditions. Labeled tRNA was visualized by autoradiography.

3. Discussion

Here, we show that MnmA, the thiouridylase in *E. coli* responsible for s²U₃₄ tRNA modifications, does not require a [4Fe-4S] cluster for activity. In contrast, when reconstituted with a [4Fe-4S] cluster, the protein was rather inactive and unable to transfer sulfur to tRNA. We show that the interaction of MnmA-rec with IscS decreased when the [4Fe-4S] cluster was present, while tRNA and ATP were still able to bind to MnmA-rec. The undetectable s²U formation originating from an Fe-S cluster reconstituted on MnmA-rec could be based on its low activity and the decreased interaction of MnmA-rec with IscS, which consequently decreased the sulfur transfer reaction (Table 1). However, this does not counter the fact that in the absence of Fe-S clusters, s²U formation was indeed detected, which further clearly showed the Fe-S cluster's independence on MnmA-catalyzed s²U formation. The presence of a [4Fe-4S] cluster in the MnmA-rec protein was verified by EPR spectroscopy, with spin relaxation properties largely reflective of a reduced [4Fe-4S]⁺ cluster. The bound Fe-S cluster exhibited largely similar g-tensor parameters to that reported preliminarily elsewhere [31,32]. Reduced [4Fe-4S]⁺ Fe-S clusters typically exhibited very fast spin relaxation properties and showed saturation only at very high microwave power and low temperatures. Both characteristics are observed in the spin relaxation of MnmA, which is largely consistent with a reduced [4Fe-4S]⁺ cluster [29]. Despite the relatively poor reduction in the bound [4Fe-4S] cluster with Na₂S₂O₄ (0.13 spins/MnmA monomer) observed, the Fe number of MnmA-rec (2.5 to 2.8 Fe/MnmA monomer) is nevertheless consistent with a majority of [4Fe-4S] clusters bound since no s²U formation was observed. Therefore, the non-Fe-S-loaded protein does not seem to perform the sulfur transfer reaction or is inactive. Our results are consistent with the grouping of *E. coli* MnmA to D-type thiouridylases, which does not bind a Fe-S cluster in the cell, while C-type MnmAs from thermophilic Archaea do [5,21]. Our data are also consistent with previous reports investigating Fe-S cluster mutants in *E. coli*, in which the s²U₃₄ tRNA modification was not impaired, but the s²C and ms²I⁶A modifications were impaired [26].

Surprisingly, in the report by Zhou et al. [29], the investigated $\Delta\text{iscUA}/\Delta\text{sufABCDSE}$ strain coincided with a complete defect in Fe-S cluster assembly in which normal $\text{mnm}^5\text{s}^2\text{U34}$ modifications were identified. This result is consistent with previous reports, showing that the $\text{mnm}^5\text{s}^2\text{U34}$ modifications are Fe-S independent [25]. However, in contrast, the authors rather interpreted this result as revealing that a yet unknown Fe-S cluster assembly pathway is responsible for providing the Fe-S clusters to MnmA in this strain [29]. We rather consider this hypothesis as unlikely since a third Fe-S cluster assembly system is not known in *E. coli*, and our data show that by reintroducing the *sufABCDSE* operon to this strain, the Fe-S cluster assembly and $\text{s}^2\text{C32}$ and $\text{ms}^2\text{i}^6\text{A37}$ modifications were restored, but not $\text{mnm}^5\text{s}^2\text{U34}$ thiomodifications. Furthermore, we tried to complement the *E. coli* ΔmnmA mutant strain with the MnmA homologs from humans, CTU1 and MTU1, that either bind Fe-S clusters or also belong to the D-type thiouridylases, respectively. While MTU1 is also Fe-S cluster-independent like MnmA [33,34], CTU1 was shown previously to carry a [3Fe-4S] cluster [20]. Nevertheless, both proteins were not able to reconstitute the *E. coli* ΔmnmA mutant strain based on their inability to bind and transfer sulfur to *E. coli* tRNA. We show that *E. coli* tRNA appears not to be bound to MTU1. The reason for the difference in tRNA remains elusive since MnmA was also unable to bind to human tRNA. We show that the sidechain mnm^5 modification does not hinder the binding to MTU1 since the tRNA without this modification was also not bound. There must be conclusively some structural differences between *E. coli* and human tRNA. The reason why some thiouridylases are Fe-S cluster-dependent while others are not remains also elusive. It might depend on the growth condition of the respective organism. When the $\text{s}^2\text{U34}$ thiomodification is synthesized under aerobic conditions, the thiomodification might easily become oxidized and exchanged by oxygen. Building an Fe-S cluster on MnmA would produce an inactive thiouridylase in the presence of oxygen in this organism; thus, the $\text{s}^2\text{U34}$ modification is inactive under aerobiosis. The cell might save energy in this way.

4. Materials and Methods

4.1. Aerobic Purification MnmA

LB medium supplemented with 50 $\mu\text{g}/\text{mL}$ of kanamycin was inoculated with either BL21 DE3 pJD69-mnmA or CL100 pJD69-mnmA. Cultures were grown overnight at 37 °C and 180 rpm. In total, 20 mL of the preculture per liter of the main culture was added to the LB medium supplemented with 50 $\mu\text{g}/\text{mL}$ of kanamycin. Cultivation continued at 37 °C and 160 rpm until $\text{OD}_{600} = 0.6$ was reached, and IPTG was added to a final concentration of 200 μM . The cultures were further incubated for 4 h at 30 °C and 160 rpm. The cells were harvested by centrifugation (5000 $\times g$, 4 °C, 5 min) and were resuspended in 50 mM HEPES, 150 mM KCl, 8.6% (v/v) glycerol, 10 mM imidazole, pH 7.5 buffer. The cell suspension was frozen at -20 °C and stored. After thawing the cells, deoxyribonuclease I (DNase I) was added at a final concentration of 1 $\mu\text{g}/\text{mL}$. The cell suspension was treated twice with a high-pressure homogenizer (CF Cell Disrupter; Constant Systems Ltd., Daventry, UK) at a pressure of 1.35 kbar. Cell debris was removed by centrifugation (20,000 $\times g$, 4 °C, 30 min). The supernatant was loaded on a column packed with a nickel-nitrilotriacetic acid (Ni-NTA) agarose resin (Macherey-Nagel GmbH; Düren, Germany) (with 0.5 mL of the resin per L culture) for affinity chromatography. The column was washed first with a 10 \times column volume of 50 mM HEPES, 150 mM KCl, 8.6% (v/v) glycerol, 10 mM imidazole, pH 7.5 buffer, followed by a wash with a 20 \times column volume of the buffer containing 20 mM imidazole. For elution, 40 mL of a 150 mM imidazole buffer was applied to the column, and fractions of 2 mL were collected. Samples of the fractions were analyzed with SDS-PAGE. After pooling the fractions containing the protein of interest, the solution was concentrated with centrifugal filters (Amicon™ Ultra-4 Centrifugal Filter Unit, molecular weight cut-off (MWCO) 30 kDa; Merck Millipore, Molsheim, France). Afterward, the buffer of the protein solution was changed to 50 mM HEPES, 150 mM KCl, 8.6% (v/v) glycerol, pH 7.5 buffer using a PD-10 column (Sephadex™ G-25 M, Cytiva, Marlborough, MA, USA). The resulting eluent was concentrated and loaded on a Superose 12 16/50 size

exclusion column (Cytiva) equilibrated in 10 mM Tris-HCl, 50 mM KCl, 12 mM Mg(OAc)₂, pH 7.5 buffer for final purification. Fractions containing MnmA were collected. The protein concentration was determined photometrically. Aliquots of the MnmA solution were frozen in liquid nitrogen and stored at $-80\text{ }^{\circ}\text{C}$.

4.2. Anaerobic Purification MnmA

The anaerobic purification of MnmA was performed as described above in an anaerobic chamber (vinyl chamber, Coy Laboratory Products Inc.; Grass Lake, MI, USA) using anaerobic buffers.

4.3. Reconstitution of MnmA with Iron–Sulfur Clusters

Reconstitution was carried out under anaerobic conditions. Reaction mixtures contained 3 μM IscS, 1 mM L-cysteine, 200 μM DTT, 1 mM FeCl₃, 25 μM PLP, and 100 μM MnmA in 1 mL. Briefly, 100 μM *E. coli* MnmA and 200 μM DTT were incubated for 30 min at 4 $^{\circ}\text{C}$ in 10 mM Tris-HCl, 300 mM NaCl, pH 9 buffer. Afterwards, 25 μM PLP was added to the mixture, followed by the addition of 1 mM L-cysteine and 1 mM FeCl₃; the reaction was continued for 4 h at 4 $^{\circ}\text{C}$. Reconstituted *E. coli* MnmA was concentrated using 30 kDa Amicon ultrafilters. The protein was then desalted into buffer containing 50 mM HEPES, 150 mM KCl, 8.6% glycerol at pH 7.5 using PD-10 filtration columns, and the protein samples with an Fe-S cofactor and a shoulder were determined by a UV spectrophotometer.

4.4. Purification of *E. coli* IscS

E. coli IscS was purified, as reported previously [35].

4.5. tRNA Extraction

RNA was extracted from *E. coli* WT and ΔiscS cells using phenol–chloroform phase separation. Chloroform was added to *E. coli* samples resuspended in a TriFast reagent at a ratio of 1:5 and was vortexed and incubated for 5 min. This was followed by centrifugation at $13,000\times g$ for 30 min at 4 $^{\circ}\text{C}$ for phase separation. The aqueous phase containing RNA was precipitated with isopropanol overnight at $-20\text{ }^{\circ}\text{C}$. The RNA pellet was recovered by centrifugation at $13,000\times g$ at 4 $^{\circ}\text{C}$ for 90 min and was then washed twice with 75% cold ethanol. Finally, the recovered RNA was dissolved in 0.3 M NaOAc at pH 4.5. RNA samples were separated using 5% urea-acrylamide gel for 1 h at 200 V. RNA bands were visualized using a Biorad gel camera following ethidium bromide staining. Corresponding tRNA bands on the gel were cut and were incubated with an RNA diffusion buffer (50 mM NaOAc, 150 mM NaCl, pH 7.0) at 4 $^{\circ}\text{C}$ overnight. tRNA samples were filtered with a 45 μM filter and precipitated with isopropanol overnight at 20 $^{\circ}\text{C}$. Samples were then centrifuged at $13,000\times g$ at 4 $^{\circ}\text{C}$ for 90 min. Pellets were then washed twice with 75% cold ethanol and were dissolved in 0.3 M NaOAc at pH 4.5. tRNA concentrations were then quantified using a NanoDrop ND-1000 spectrophotometer (Thermo Fisher Scientific; Wilmington, DE, USA).

4.6. Surface Plasmon Resonance (SPR) Measurements

For the binding experiments using the SPR-based method, a Biacore™ T200 instrument was employed using CM5 sensor chips at a temperature of 25 $^{\circ}\text{C}$ and a flow rate of 30 mL/min. For data evaluation, the Biacore control T200 software and evaluation T200 software were used (Cytiva; Marlborough, MA, USA). The autosampler rack was at 8 $^{\circ}\text{C}$ to cool the samples. Proteins for each immobilization were obtained from independent purifications. The running buffer containing 20 mM phosphate, 150 mM NaCl, 0.005% (*v/v*) Tween 20, pH 7.4 was employed. Analytes with concentrations of 0.16, 0.31, 0.63, 1.25, 2.5, 5, 10, and 20 μM were injected for 4.5 min at a flow rate of 30 mL/min followed by a 15 min dissociation and regeneration of the sensor surface with 50 mM of HCl for 1 min. Bovine serum albumin (BSA) served as a negative control ligand. Binding curves for both flow cells were corrected by the subtraction of buffer injection curves.

4.7. In Vitro tRNA Thiolation Assay

For in vitro s²U formation, 1 mM of L-cysteine, 100 μM IscS and 150 μM *E. coli* MnmA were used in the presence of 1 mM DTT, 1 mM ATP, 20 μM PLP and 300 μg tRNA in a total reaction volume of 500 μL with 10 mM Tris-HCl, 50 mM KCl, 12 mM Mg(OAc)₂, and pH 7.5 buffer. The mixture was incubated at 37 °C for 2 h. The same procedure was repeated anaerobically in the glove box for anaerobically purified MnmA. After the completion of the reactions, tRNA was recovered by the tRNA extraction procedure described above.

4.8. HPLC Analysis

In total, 200 μg of tRNA in 50 mM NaOAc, 30 mM ZnOAc, pH 5.3 buffer was digested with P1 nuclease (1 μL per 50 μg of tRNA) and was incubated at 42 °C overnight. In total, 13 μL of 1 M of unbuffered Tris was added, followed by FastAP (1 μL/50 μg), and incubation was continued at 42 °C overnight. Samples were loaded in HPLC vials and analyzed using the LiChrospher[®] RP-18 column, following a stepwise gradient program as described by Gehrke to quantify the nucleosides. [36].

4.9. Trypsinolysis Assay

The method was adopted with modifications from Kambampati and Lauhon [15]. The proteolytic digestion of MnmA and MTU1 with trypsin was conducted in 10mM Tris-HCl, 50 mM KCl, 12 mM Mg(OAc)₂, pH 7.5 buffer with a final volume of 100 μL. A total of 0.13 mg/mL MnmA (3.17 μM) was preincubated with a 1.5 mg/mL bulk of tRNA purified from *ΔiscS* or *ΔMOCS3* knock-out cells [37] (human embryonic kidney cells (HEK) 293T) and 1 mM of ATP at 37 °C for 5 min. Cleavage was started by adding trypsin (TPCK treated from bovine pancreas with a 12,500 U/mg protein, Sigma) with a final concentration of 2.6 μg/mL or 6.5 μg/mL, which corresponds to a MnmA/trypsin ratio of either 50:1 (*w/w*) or 20:1 (*w/w*), respectively. Cleavage samples were incubated at 37 °C for 1 h. At 0, 5, 10, 20, 30, and 60 min, 15 μL aliquots containing approximately 2 μg MnmA were taken from the reaction mixtures, and a 5 μL 4 × SDS loading buffer was added to stop the reaction. Afterward, the samples were analyzed by SDS-PAGE (method 2.4.10) with 10% acrylamide gels.

4.10. In Vitro AMP Formation

To demonstrate the adenylation of the tRNA by His₁₀-MnmA and thus the indirect binding of the ribonucleic acid to the protein, 20 μM tRNA (isolated from *ΔiscS*) was incubated with 20 μM MnmA as well as 250 μM ATP, 250 μM MgCl₂ and 2 U PP_i in a volume of 300 μL with 100 mM of Tris-HCl at pH 7.2 for a period of 2 h at room temperature. The reaction was stopped by adding 1% (*w/v*) SDS. The samples were then heat-denatured for 15 min at 95 °C and were then centrifuged in Amicon Ultra 0.5 concentrators for 1 h at 14,000× *g* and 0 °C. The AMP formed during the reaction was applied in 50 mM of (NH₄)₂HPO₄ at pH 2.5 with 2% MeOH on a HPLC C18 RP column (Hypersil-ODS-Particle, 5 μm, 250 × 4.6 mm). Detection was performed at 260 nm.

4.11. In Vitro Thiolation Labeling of tRNA

Purified tRNA from *ΔiscS* was radiolabeled with L-³⁵S-cysteine for sulfur transfer to tRNA. Briefly, 10 μCi L-³⁵S-cysteine, 100 μM IscS and 150 μM of *E. coli* MnmA were incubated in the presence of 1 mM DTT, 1mM ATP, 20 μM PLP and 300 μg tRNA in a total reaction volume of 50 μL of 10 mM Tris, 50 mM KCl, 12 mM Mg(OAc)₂, pH 7.5 buffer. The mixture was incubated at 37 °C for 2 h. The tRNA was isolated using phenol–chloroform phase separation (chloroform/Trifast (1:5)), which was vortexed and incubated for 5 min. This was followed by centrifugation at 13,000× *g* for 30 min at 4 °C for phase separation. The aqueous phase containing RNA was precipitated with isopropanol overnight at −20 °C. The RNA pellet was recovered by centrifugation at 13,000× *g* at 4 °C for 90 min and was then washed twice with 75% cold ethanol. Finally, the recovered RNA was dissolved in 0.3 M NaOAc, pH 4.5 buffer. RNA samples were separated into 5% urea-acrylamide gels

for 1 h at 200 V. The radioactivity on the gel was transferred onto a membrane overnight, and a picture of radiolabeled tRNA was taken.

4.12. Electron Paramagnetic Resonance (EPR) Spectroscopy

To characterize the Fe-S cluster bound to MnmA, EPR samples were prepared anaerobically in a Coy chamber ($O_2 < 50$ ppm) at 4 °C in a thermoblock in a 10 mM Tris-HCl, 50 mM KCl, 12 mM $MgCl_2$, buffer at pH 8.5. To 72 μ L of 275 μ M MnmA-rec (as obtained with a light, yellowish-black hue), 8 μ L of 100 mM $Na_2S_2O_4$ was added, which, upon mixing, resulted in a very slight but observable color change. The sample was incubated for 30 min with a reductant at 4 °C before loading the mixture into a quartz EPR capillary (3.9 mm outer diameter; QSIL SE, Langewiesen, Germany) and freezing in a liquid N_2 -cooled ethanol bath, and before complete freezing in liquid N_2 . Continuous wave X-band EPR spectra were obtained on a laboratory-built spectrometer equipped with a Bruker SHQ resonator with an ESR 910 helium flow cryostat and an ITC503 temperature controller (Oxford Instruments; Abingdon, UK). Instrument components of the laboratory-built spectrometer included an ER041MR microwave bridge (Bruker), an SR810 lock-in amplifier (Stanford Research Systems; Sunnyvale, CA, USA), and a 53181A microwave counter (Agilent Technologies; Santa Clara, CA, USA). A Cu(II)-EDTA standard was used as a reference for the spin quantitation of the MnmA Fe-S cluster, while routine magnetic field calibrations were used to compensate field offsets between the Hall probe and the sample position was performed by measuring a reference $N@C_{60}$ sample at ambient temperature [38,39]. Spin quantitation was performed via double integration using the utility ‘spincounting’ (<https://github.com/lcts/spincounting>, accessed on 23 July 2022) in Matlab R2023a. The spectral simulation of the bound Fe-S cluster was performed using the EasySpin simulation package (version 6.0.0-dev.48) in Matlab R2023a (The Mathworks; Natick, MA, USA) [31,40]. An analysis of the power dependence of the MnmA-reduced Fe-S cluster was performed by plotting $\log(S/\sqrt{P})$ vs. $\log P$ using the intensity of the signal feature at 3530 G. Paramagnetic signals that do not show power saturation effects result in plots that are parallel to the abscissa with power saturation effects that exhibit a slope toward the abscissa with increasing power [31]. P_M , $P_{1/2}$, and b were estimated by fitting the plot to the equation $S = \sqrt{P/(1 + P/P_{1/2})}^{0.5b}$.

4.13. Quantification of Fe Content

The iron content was determined for purified MnmA proteins by inductively coupled plasma–optical emission spectroscopy (ICP-OES) after published procedures [41].

5. Conclusions

E. coli MnmA so far has been believed to be an Fe-S cluster-independent protein based on the fact that no Fe-S cluster has been identified in the crystal structure of the protein [16,17]. However, a recent report described the purification of a [4Fe-4S] cluster containing the MnmA protein isolated under anaerobic conditions from *E. coli* and reported that this [4Fe-4S] cluster is essential for the activity of MnmA [29]. In total, this report contradicts previously published data, where it is shown that by using an *E. coli iscS* mutant strain complemented with a *sufS*-expressing plasmid, the Fe-S cluster biosynthesis can be rescued in this strain, and the strain is able to produce s^2C32 or ms^2i^6A37 -modified tRNAs, but not s^4U8 and (c)mnm⁵ s^2U34 tRNAs [26].

In this report, we aimed to dissect the controversy of whether the *E. coli* MnmA protein is an Fe-S cluster-dependent or independent protein. In our hands, we showed that when Fe-S clusters are bound to MnmA, tRNA thiolation is inhibited since MnmA is unable to transfer the sulfur to the bound tRNA, thereby making MnmA an Fe-S cluster-independent protein. We further show the 2-thiouridylase only binds tRNA from its own organism.

Author Contributions: Conceptualization, S.L.; methodology, B.R.D.; validation, M.O., L.W. and E.A.F.; investigation M.O., L.W. and E.A.F.; resources, S.L.; data curation, M.O., L.W. and E.A.F.; writing—original draft preparation, S.L.; writing—review and editing, B.R.D. and M.O.; visualization,

M.O.; supervision, S.L.; project administration, S.L.; funding acquisition, S.L. All authors have read and agreed to the published version of the manuscript.

Funding: This work was funded by the Deutsche Forschungsgemeinschaft (DFG) priority program SPP1927 grant LE1171/15-2.

Data Availability Statement: Data are available upon request.

Acknowledgments: We thank Beatrice Py for providing strain Δ iscUA/ Δ sufABCDSE. We thank Angelika Lehmann (University of Potsdam) for help with the Biacore experiment, and Christian Teutloff and Robert Bittl (FU Berlin) for help with the EPR experiment.

Conflicts of Interest: The authors declare no conflicts of interest.

References

1. Grosjean, H.; de Crecy-Lagard, V.; Marck, C. Deciphering synonymous codons in the three domains of life: Co-evolution with specific tRNA modification enzymes. *FEBS Lett.* **2010**, *584*, 252–264. [[CrossRef](#)]
2. Leimkühler, S.; Böhning, M.; Beilschmidt, L. Shared Sulfur Mobilization Routes for tRNA Thiolation and Molybdenum Cofactor Biosynthesis in Prokaryotes and Eukaryotes. *Biomolecules* **2017**, *7*, 5. [[CrossRef](#)]
3. Agris, P.F.; Narendran, A.; Sarachan, K.; Vare, V.Y.P.; Eruysal, E. The Importance of Being Modified: The Role of RNA Modifications in Translational Fidelity. *Enzymes* **2017**, *41*, 1–50. [[CrossRef](#)] [[PubMed](#)]
4. Rezgui, V.A.; Tyagi, K.; Ranjan, N.; Konevega, A.L.; Mittelstaet, J.; Rodnina, M.V.; Peter, M.; Pedrioli, P.G. tRNA tKUUU, tQUUG, and tEUUC wobble position modifications fine-tune protein translation by promoting ribosome A-site binding. *Proc. Natl. Acad. Sci. USA* **2013**, *110*, 12289–12294. [[CrossRef](#)] [[PubMed](#)]
5. Shigi, N. Biosynthesis and functions of sulfur modifications in tRNA. *Front. Genet.* **2014**, *5*, 67. [[CrossRef](#)] [[PubMed](#)]
6. Leidel, S.; Pedrioli, P.G.; Bucher, T.; Brost, R.; Costanzo, M.; Schmidt, A.; Aebersold, R.; Boone, C.; Hofmann, K.; Peter, M. Ubiquitin-related modifier Urm1 acts as a sulphur carrier in thiolation of eukaryotic transfer RNA. *Nature* **2009**, *458*, 228–232. [[CrossRef](#)]
7. Asano, K.; Suzuki, T.; Saito, A.; Wei, F.Y.; Ikeuchi, Y.; Numata, T.; Tanaka, R.; Yamane, Y.; Yamamoto, T.; Goto, T.; et al. Metabolic and chemical regulation of tRNA modification associated with taurine deficiency and human disease. *Nucleic Acids Res.* **2018**, *46*, 1565–1583. [[CrossRef](#)] [[PubMed](#)]
8. Suzuki, T. The expanding world of tRNA modifications and their disease relevance. *Nat. Rev. Mol. Cell Biol.* **2021**, *22*, 375–392. [[CrossRef](#)] [[PubMed](#)]
9. Nedialkova, D.D.; Leidel, S.A. Optimization of Codon Translation Rates via tRNA Modifications Maintains Proteome Integrity. *Cell* **2015**, *161*, 1606–1618. [[CrossRef](#)] [[PubMed](#)]
10. Armengod, M.E.; Meseguer, S.; Villarroya, M.; Prado, S.; Moukadiri, I.; Ruiz-Partida, R.; Garzon, M.J.; Navarro-Gonzalez, C.; Martinez-Zamora, A. Modification of the wobble uridine in bacterial and mitochondrial tRNAs reading NNA/NNG triplets of 2-codon boxes. *RNA Biol.* **2014**, *11*, 1495–1507. [[CrossRef](#)]
11. Rozov, A.; Demeshkina, N.; Khusainov, I.; Westhof, E.; Yusupov, M.; Yusupova, G. Novel base-pairing interactions at the tRNA wobble position crucial for accurate reading of the genetic code. *Nat. Commun.* **2016**, *7*, 10457. [[CrossRef](#)] [[PubMed](#)]
12. Durant, P.C.; Bajji, A.C.; Sundaram, M.; Kumar, R.K.; Davis, D.R. Structural effects of hypermodified nucleosides in the *Escherichia coli* and human tRNA^{Lys} anticodon loop: The effect of nucleosides s²U, mcm⁵U, mcm⁵s²U, mnm⁵s²U, t⁶A, and ms²t⁶A. *Biochemistry* **2005**, *44*, 8078–8089. [[CrossRef](#)] [[PubMed](#)]
13. Nilsson, K.; Jager, G.; Bjork, G.R. An unmodified wobble uridine in tRNAs specific for Glutamine, Lysine, and Glutamic acid from *Salmonella enterica* Serovar Typhimurium results in nonviability-Due to increased missense errors? *PLoS ONE* **2017**, *12*, e0175092. [[CrossRef](#)] [[PubMed](#)]
14. Ikeuchi, Y.; Shigi, N.; Kato, J.; Nishimura, A.; Suzuki, T. Mechanistic insights into sulfur relay by multiple sulfur mediators involved in thiouridine biosynthesis at tRNA wobble positions. *Mol. Cell* **2006**, *21*, 97–108. [[CrossRef](#)] [[PubMed](#)]
15. Kambampati, R.; Lauhon, C.T. MnmA and IscS are required for in vitro 2-thiouridine biosynthesis in *Escherichia coli*. *Biochemistry* **2003**, *42*, 1109–1117. [[CrossRef](#)]
16. Numata, T.; Ikeuchi, Y.; Fukai, S.; Suzuki, T.; Nureki, O. Snapshots of tRNA sulphuration via an adenylated intermediate. *Nature* **2006**, *442*, 419–424. [[CrossRef](#)] [[PubMed](#)]
17. Numata, T.; Ikeuchi, Y.; Fukai, S.; Adachi, H.; Matsumura, H.; Takano, K.; Murakami, S.; Inoue, T.; Mori, Y.; Sasaki, T.; et al. Crystallization and preliminary X-ray analysis of the tRNA thiolation enzyme MnmA from *Escherichia coli* complexed with tRNA^{Glu}. *Acta Crystallogr. Sect. F Struct. Biol. Cryst. Commun.* **2006**, *62*, 368–371. [[CrossRef](#)]
18. Moukadiri, I.; Garzon, M.J.; Bjork, G.R.; Armengod, M.E. The output of the tRNA modification pathways controlled by the *Escherichia coli* MnmEG and MnmC enzymes depends on the growth conditions and the tRNA species. *Nucleic Acids Res.* **2014**, *42*, 2602–2623. [[CrossRef](#)]
19. Sasarman, F.; Antonicka, H.; Horvath, R.; Shoubridge, E.A. The 2-thiouridylase function of the human MTU1 (TRMU) enzyme is dispensable for mitochondrial translation. *Hum. Mol. Genet.* **2011**, *20*, 4634–4643. [[CrossRef](#)]

20. Liu, Y.; Vinyard, D.J.; Reesbeck, M.E.; Suzuki, T.; Manakongtreecheep, K.; Holland, P.L.; Brudvig, G.W.; Soll, D. A [3Fe-4S] cluster is required for tRNA thiolation in archaea and eukaryotes. *Proc. Natl. Acad. Sci. USA* **2016**, *113*, 12703–12708. [[CrossRef](#)]
21. Shigi, N.; Suzuki, T.; Terada, T.; Shirouzu, M.; Yokoyama, S.; Watanabe, K. Temperature-dependent biosynthesis of 2-thioribothymidine of *Thermus thermophilus* tRNA. *J. Biol. Chem.* **2006**, *281*, 2104–2113. [[CrossRef](#)]
22. Noma, A.; Shigi, N.; Suzuki, T. Biogenesis and Functions of Thio-Compounds in transfer RNA: Comparison of bacterial and eukaryotic thiolation machineries. In *DNA and RNA Modification Enzymes*; Landes Bioscience: Austin, TX, USA, 2009; pp. 392–405.
23. Maynard, N.D.; Macklin, D.N.; Kirkegaard, K.; Covert, M.W. Competing pathways control host resistance to virus via tRNA modification and programmed ribosomal frameshifting. *Mol. Syst. Biol.* **2012**, *8*, 567. [[CrossRef](#)]
24. Leiva, L.E.; Pincheira, A.; Elgamal, S.; Kienast, S.D.; Bravo, V.; Leufken, J.; Gutierrez, D.; Leidel, S.A.; Ibba, M.; Katz, A. Modulation of *Escherichia coli* Translation by the Specific Inactivation of tRNA(Gly) Under Oxidative Stress. *Front. Genet.* **2020**, *11*, 856. [[CrossRef](#)]
25. Suzuki, T. Biosynthesis and function of tRNA wobble modifications. *Top. Curr. Genet.* **2005**, *12*, 23–69.
26. Bühning, M.; Valleriani, A.; Leimkühler, S. The Role of SufS Is Restricted to Fe-S Cluster Biosynthesis in *Escherichia coli*. *Biochemistry* **2017**, *56*, 1987–2000. [[CrossRef](#)] [[PubMed](#)]
27. Bouvier, D.; Labessan, N.; Clemancey, M.; Latour, J.M.; Ravanat, J.L.; Fontecave, M.; Atta, M. TtcA a new tRNA-thioltransferase with an Fe-S cluster. *Nucleic Acids Res.* **2014**, *42*, 7960–7970. [[CrossRef](#)]
28. Mulliez, E.; Duarte, V.; Arragain, S.; Fontecave, M.; Atta, M. On the Role of Additional [4Fe-4S] Clusters with a Free Coordination Site in Radical-SAM Enzymes. *Front. Chem.* **2017**, *5*, 17. [[CrossRef](#)] [[PubMed](#)]
29. Zhou, J.; Lenon, M.; Ravanat, J.L.; Touati, N.; Velours, C.; Podskocznyj, K.; Leszczynska, G.; Fontecave, M.; Barras, F.; Golinelli-Pimpaneau, B. Iron-sulfur biology invades tRNA modification: The case of U34 sulfuration. *Nucleic Acids Res.* **2021**, *49*, 3997–4007. [[CrossRef](#)] [[PubMed](#)]
30. Freibert, S.A.; Weiler, B.D.; Bill, E.; Pierik, A.J.; Muhlenhoff, U.; Lill, R. Biochemical Reconstitution and Spectroscopic Analysis of Iron-Sulfur Proteins. *Methods Enzym.* **2018**, *599*, 197–226. [[CrossRef](#)]
31. Rupp, H.; Rao, K.K.; Hall, D.O.; Cammack, R. Electron spin relaxation of iron-sulfur proteins studied by microwave power saturation. *Biochim. Biophys. Acta* **1978**, *537*, 255–269. [[CrossRef](#)] [[PubMed](#)]
32. Guigliarelli, B.; Bertrand, P. Application of EPR spectroscopy to the structural and functional study of iron-sulfur proteins. *Adv. Inorg. Chem.* **1999**, *47*, 421–497. [[CrossRef](#)]
33. Umeda, N.; Suzuki, T.; Yukawa, M.; Ohya, Y.; Shindo, H.; Watanabe, K. Mitochondria-specific RNA-modifying enzymes responsible for the biosynthesis of the wobble base in mitochondrial tRNAs. Implications for the molecular pathogenesis of human mitochondrial diseases. *J. Biol. Chem.* **2005**, *280*, 1613–1624. [[CrossRef](#)]
34. Wu, Y.; Wei, F.Y.; Kawarada, L.; Suzuki, T.; Araki, K.; Komohara, Y.; Fujimura, A.; Kaitsuka, T.; Takeya, M.; Oike, Y.; et al. Mtu1-Mediated Thiouridine Formation of Mitochondrial tRNAs Is Required for Mitochondrial Translation and Is Involved in Reversible Infantile Liver Injury. *PLoS Genet.* **2016**, *12*, e1006355. [[CrossRef](#)]
35. Leimkühler, S.; Rajagopalan, K.V. An *Escherichia coli* NifS-like sulfurtransferase is required for the transfer of cysteine sulfur in the in vitro synthesis of molybdopterin from precursor Z. *J. Biol. Chem.* **2001**, *276*, 22024–22031. [[CrossRef](#)]
36. Gehrke, C.W.; Kuo, K.C. Ribonucleoside analysis by reversed-phase high-performance liquid chromatography. *J. Chromatogr.* **1989**, *471*, 3–36. [[CrossRef](#)]
37. Ogunkola, M.O.; Guiraudie-Capraz, G.; Feron, F.; Leimkühler, S. The Human Mercaptopyruvate Sulfurtransferase TUM1 Is Involved in Moco Biosynthesis, Cytosolic tRNA Thiolation and Cellular Bioenergetics in Human Embryonic Kidney Cells. *Biomolecules* **2023**, *13*, 144. [[CrossRef](#)]
38. Weidinger, A.; Waiblinger, M.; Pietzak, B.; Murphy, T.A. Atomic nitrogen in C₆₀: N@C₆₀. *Appl. Phys. A* **1998**, *66*, 287–292. [[CrossRef](#)]
39. Wittmann, J.J.; Can, T.V.; Eckardt, M.; Harneit, W.; Griffin, R.G.; Corzilius, B. High-precision measurement of the electron spin g factor of trapped atomic nitrogen in the endohedral fullerene N@C₆₀. *J. Magn. Reson.* **2018**, *290*, 12–17. [[CrossRef](#)] [[PubMed](#)]
40. Stoll, S.; Schweiger, A. EasySpin, a comprehensive software package for spectral simulation and analysis in EPR. *J. Magn. Reson.* **2006**, *178*, 42–55. [[CrossRef](#)] [[PubMed](#)]
41. Neumann, M.; Leimkühler, S. Heavy metal ions inhibit molybdoenzyme activity by binding to the dithiolene moiety of molybdopterin in *Escherichia coli*. *FEBS J.* **2008**, *275*, 5678–5689. [[CrossRef](#)] [[PubMed](#)]

Disclaimer/Publisher’s Note: The statements, opinions and data contained in all publications are solely those of the individual author(s) and contributor(s) and not of MDPI and/or the editor(s). MDPI and/or the editor(s) disclaim responsibility for any injury to people or property resulting from any ideas, methods, instructions or products referred to in the content.